**Received:** 12 April 2025 | **Revised:** 15 June 2025 | **Accepted:** 26 June 2025 Science Research Annals—Physical Sciences 1(1), 24–33

SCIENCE RESEARCH ANNALS
(PHYSICAL SCIENCES)

Published by Faculty of Science, Adekunle Ajasin University, Akungba-Akoko (AAUA)

Journal website: https://sra.com.ng/index.php/sra-physical

SCIENTIFIC ARTICLE DOI: https://doi.org/10.63112/e79ke582

# A combined interpretation of electrical resistivity and airborne magnetic datasets for assessment and evaluation of a geothermal reservoir in South West Nigeria

Samuel O. Sedara [1, *]

[1] *Department of Physics and Electronics, Faculty of Science, Adekunle Ajasin University, 001 Akungba-Akoko, Ondo State, Nigeria*

*Correspondence: samuel.sedara@aaua.edu.ng (S.O. Sedara)

**ARTICLE INFORMATION**

***Keywords:***
Electrical resistivity
Aeromagnetic data
Ikogosi warm spring
Geothermal energy
Curie point depth
Heat flow

**Handling Editor:** M.B. Aminu

**Disclaimer:** All opinions expressed are solely the authors, and do not necessarily represent that of the Journal's Editorial Board, Management, or workers.

**License:** SRA, AAUA, Nigeria.

**ABSTRACT**

The surface occurrence and manifestation of warm and hot springs in a location are of utmost concern and require preliminary investigation to ascertain the reasons for this natural event. This event has also been observed in some other parts of Nigeria. So, the Ikogosi Warm Spring (IKGWS) area and environs were chosen as a study site located in the southwestern part of Nigeria because of their proximity. Thus, the causes and sources of the flow of hot and cold springs manifested on the surface in the area were explored. In this work, a combination of two geophysical techniques was used to describe and understand the configuration and processes of this typical event. The method involved the acquisition of resistivity data using a Terrameter (ABEM SAS 300C) from nine (9) vertical electrical soundings (VES) stations and supported by airborne magnetic data from the warm and cold sections of the study area. The VES analysis shows that the subsurface is made of four to six layers with resistivity ranging from 1.0 to 1334.7 Ωm. It also revealed that VES 1, 2 and 3 has resistivity ranging from 62.5-1082.8 Ωm with depths between 0.7-58.8 m and thickness 0.7-45.7 m while VES 4, 5 and 6 has resistivity ranging from 83.7-1334.7 Ωm with depth between 0.6-30.6 m and thickness 0.6-18.3 m. The general distribution of resistivity shows a very low value near the Ikogosi spring, revealing that resistivity ranged from 1 to 2540.3 Ωm, depth: 0.6 to 112.3 m, and thickness: 0.7 to 66.8 m. The results from heat flow computation from aeromagnetic investigations confirmed that there are zones in the IKGWS with anomalous heat flow, which have great prospects for geothermal energy exploration. The heat flow estimated for the IKGWS and environs ranged between 75 and 127 mW/m$^{2,}$ and the average value of 100 mW/m$^{2,}$ while the temperature gradient varied between 28 and 48 °C/Km and the mean value of 38 °C/Km. Likewise, the Curie point depth (CPD) estimated ranged between 12 and 21 km and mean value of 16 km.

## Highlights

- An Integrated geophysical study comprising resistivity and aeromagnetic data was used to evaluate the Ikogosi Warm Spring's geothermal potential, revealing subsurface structures and fluid pathways.
- The resistivity data identified 4-6 subsurface layers with resistivity ranging 1.0–2540.3 Ωm, delineating conductive fractured quartzite zones (1–658 Ωm) as primary geothermal fluid conduits.
- The aeromagnetic data estimated a Curie Point Depth (CPD) of 12–21 km (with mean value of 16 km) and heat flow values of 75–127 mW/m² (with mean value of 100 mW/m²), indicating anomalous crustal thermal gradients (28–48°C/km) and viable geothermal resources.
- Fault-controlled permeability governs and facilitates fluid migration and ascent, with geochemical evidence suggesting a hybrid (magmatic and meteoric) origin for the geothermal springs.

**Copyright:** © 2025 by the authors. Authors could also grant permission to third parties freely, as long as adequate reference is made to the original SRA-P article. This article is an open access article distributed under the terms and conditions of the Creative Commons Attribution (CC BY) license (https://creativecommons.org/lincenses/by/4.0/).

## 1. Introduction

Geothermal power deposition can be found in an area only if it is characterized by the existence of a source of natural heat of great output, such as cooling magma, an adequate water supply, an aquifer or permeable reservoir, and an impermeable cap rock. The Ikogosi Warm Spring (IKGWS) is assumed to possess all these geothermal energy characteristics. There are hot and cold springs tributaries in Ikogosi Warm Spring, which is located in the southwestern part of Nigeria. Geothermal resource viability requires three synergistic components: (1) an active heat anomaly (typically >70°C/km gradient) from magmatic intrusions or radiogenic crust (Fridleifsson et al., 2021), (2) a fractured reservoir with >10% porosity for fluid circulation (Grant and Bixley, 2023), and (3) a low-permeability seal (e.g., clay-rich strata) to prevent thermal dissipation (Aneke et al., 2022). The genesis of thermal springs remains contested between magmatic fluid exsolution (evidenced by $\delta^{18}O$ isotopic signatures in Andrés et al., 2020) and deep percolation of meteoric water heated via crustal thermal decay (Battistel et al., 2021).

There are many natural origin of springs that needed to be investigated in which scientific postulate focused on one of two alternatives of whether the waters rise from hot magmas at depth that flows from Precambrian rocks (migmatite – gneiss) or they are original rain water which has percolated down deep into the earth's crust, thereby heated by some unknown process (Garba et al., 2012; Hairul et al., 2013). The Ikogosi Spring system (SW Nigeria) exemplifies this duality, exhibiting: Coexisting 70°C hot and 25°C cold springs (Olabode, 2023), Discharge rates of 5-8 L/s suggesting fault-controlled permeability (Adagunodo et al., 2022), Geochemical evidence of both magmatic (elevated Li/Si ratios) and meteoric (low $Cl^-$) components (Ehinola et al., 2021). Recent magnetotelluric surveys reveal a 3.5 km deep conductive zone (>100 Ωm) beneath Ikogosi, potentially indicating an active heat source (Abdullahi et al., 2023). This aligns with global observations of hybrid geothermal systems in Precambrian terranes (Mielke et al., 2022).

Information about aquifers, water tables, salinities, impermeable formations, bedrock, etc, can be obtained from resistivity and magnetic surveys. This study aims to characterize the hydrothermal and hydrogeological properties of the spring water sources and determine the depth to proximal aquifers/reservoirs through integrated geophysical analysis. By employing resistivity surveys and airborne magnetic data, we seek to: (1) establish the geothermal signature of the study area, and (2) elucidate the genetic origins of the thermal springs. While these methods have traditionally been applied to groundwater potential assessments and hydro-chemical analyses, their utility extends to multiple subsurface investigations including: Delineation of saturated zones and water table depth, Mapping of weathered layer thicknesses, Identification of structural discontinuities (fractures, faults, fissures), Determination of aquifer geometry (lateral extent, thickness), Analysis of groundwater flow dynamics, Characterization of basement topography in crystalline terrains, Detection of freshwater/saltwater interfaces, Mineral prospecting and archaeological investigations. The methodology offers particular advantages for foundational hydrogeological studies due to its portability (Field equipment is highly mobile and adaptable), versatility (Capable of detecting both lithological contrasts (resistivity) and magnetic susceptibility variations), and precision, which provides quantitative data on aquifer properties, bedrock depth, and impermeable layer distribution. The apparent resistivity ($\rho_a$), which represents the measured parameter in both laboratory and field settings, is defined as:

$$\rho_a = k(\Delta V/I) \quad (1)$$

where: k = geometric factor (m), ΔV = potential difference (V), I = current (A)

This formulation serves as the fundamental basis for interpreting subsurface conductivity structures, with true resistivity requiring additional inversion modeling to account for anisotropic effects. The primary objective of Direct Current (DC) electrical surveys is to characterize subsurface resistivity distributions through direct current measurements. These methods have demonstrated long-term efficacy in geothermal investigations, employing various electrode configurations to delineate system boundaries at shallow depths (<500 m) (Allis, 1990; Meidav, 1998). Resistivity techniques are particularly valuable in geothermal exploration due to their sensitivity to key reservoir properties, which re temperature variations (↓ resistivity with ↑ temperature), pore fluid salinity, rock porosity, and clay content. These parameters create distinct resistivity contrasts between high-temperature zones (typically 5-50 Ωm), cold groundwater systems (often >100 Ωm), and clay cap formations (1-10 Ωm) (Arnason et al., 2010). This study presents integrated resistivity and aeromagnetic results from the Ikogosi warm spring region. The Vertical Electrical Sounding (VES) used the Configuration of Schlumberger array **(**AMNB electrode layout) because of its optimal vertical resolution for layered geology, reduced potential electrode movement requirements, and enhanced signal-to-noise ratio at greater spacings (Zonge et al., 2005). The Apparent resistivity ($\rho_a$) was derived using:

$$\rho_a = \pi \frac{\left[\left(\frac{AB}{2}\right)^2 - \left(\frac{MN}{2}\right)^2\right]}{MN} \times \left(\frac{\Delta V}{I}\right) \quad (2)$$

where: AB = current electrode spacing (m), MN = potential electrode spacing (m), ΔV = measured potential difference (V), I = injected current (A)

The resistivity structure of geothermal reservoirs exhibits consistent patterns globally, particularly in relation to temperature-controlled alteration zones (Figure 1). A well-defined resistivity zonation—comprising a conductive clay cap underlain by a resistive high-temperature core—has been documented across diverse geological settings (Árnason et al., 2000; Ussher et al., 2000; Anderson et al., 2000). This conceptual model reliably applies to systems with high permeability and pervasive hydrothermal alteration. Deviations from this pattern typically indicate irregular permeability distributions, disequilibrium between rock and fluid chemistry (Flovenz et al., 2005). There are key resistivity-temperature relationships in Vapor-Dominated Systems which exhibit higher resistivity (>100 Ωm) in steam-rich zones (Arnason et al., 2010) and lithological controls where resistivity ranges vary with host rock composition (e.g., volcanic vs. sedimentary) and alteration in mineralogy (smectite, illite, chlorite) which further modifies conductivity (Ussher et al., 2000). While permeability remains inherently uncertain, targeting resistivity anomalies improves drilling success rates by identifying thermally active zones, delineating clay cap boundaries (typically 5–20 Ωm), and avoiding overcooled or mineralized regions. Local geological heterogeneity (e.g., fault-controlled fluid flow) may override regional trends, necessitating integrated magnetotelluric/geochemical surveys (Cumming et al., 2020).

Geothermal systems exhibit distinct electrical properties that make them ideal targets for electromagnetic exploration methods. In thermal

areas, the resistivity is substantially different from and generally lower than in areas with colder subsurface temperatures. The resistivity is affected by the vertically ascending, hot, and mineralized hydrothermal waters that have their origin in the mix of descending surface waters and ascending deep waters. The resistivity of porous media within this system is a function of matrix resistivity, fluid resistivity and saturation, temperature, and porosity. The empirical relationship between resistivity ρ, porosity ɵ, water saturation Sw, and fluid resistivity ρw, given by Archie (1942) in Eq. 3:

$$\rho = a \cdot \rho_w \cdot \varphi^{-m} \cdot S_w^{-n} \quad (3)$$

where: ρ = bulk resistivity (Ωm), $\rho_w$ = pore fluid resistivity (Ωm), φ = porosity (fraction), $S_w$ = water saturation (fraction), a = tortuosity factor (typically 0.5-2.5),m = cementation exponent (1.8-2.5 for sandstones), n = saturation exponent (≈2).

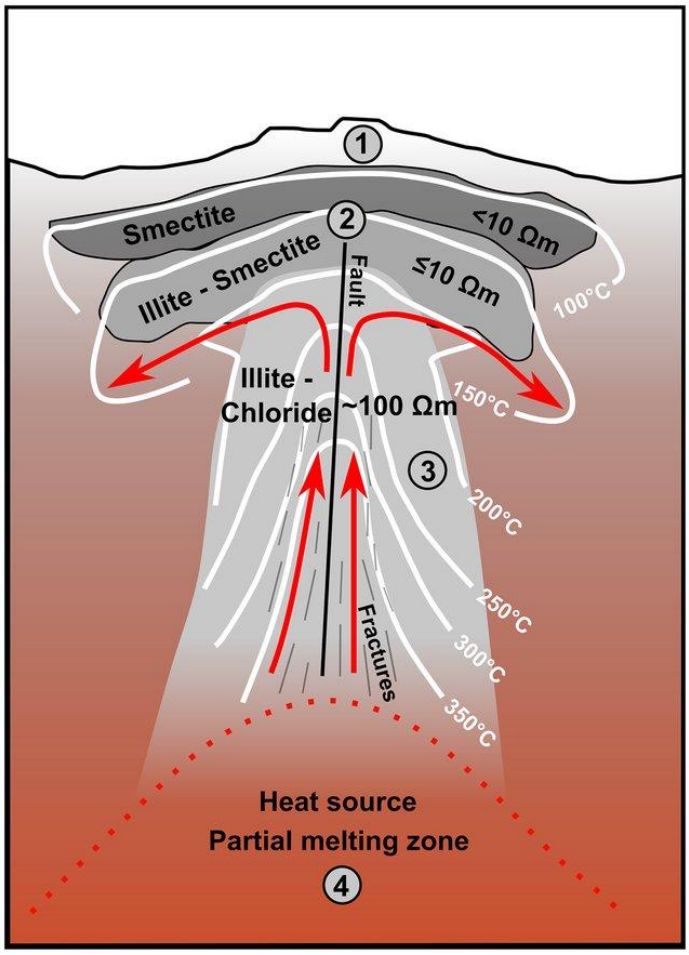


**Figure 1:** Resistivity model of a typical geothermal reservoir (Samrock et al, 2015).

## 2. Geological Background and Location of the Study Area

The Ikogosi geothermal feature is situated in Ekiti State, southwestern Nigeria (7°35'30"-7°35'45"N, 4°58'45"-4°58'54"E), within the ancient Precambrian basement complex. This geological province consists primarily of highly metamorphosed rocks, forming part of Nigeria's extensive schist belt system. The local stratigraphy belongs to the undifferentiated post-Cretaceous basement complex, dominated by shale and sandstone formations (Adegbuyi and Abimbola, 1997). This low-enthalpy thermal system exhibits dual spring discharges with distinct temperature regimes, i.e., cold springs maintaining 25-35°C and warm springs ranging 38.5-40.1°C (based on recent field measurements). The geothermal system's heat source remains uncharacterized, though its surface expressions suggest fracture-controlled hydrothermal circulation. Three principal quartzite lithologies have been identified in the area, which are massive quartzite formations, fissile quartzite layers, and interbedded mica and quartz schists (Caby and Boesse, 2001). The regional structural features include concealed fault zones and shear systems, with observable fracturing occurring primarily along fluvial valleys, at elevated topographic positions, and within limited outcrop exposures (Figure 2).

## 3. Methodology

### *3.1 Geophysical Survey Methodology*

#### *3.1.1 Electrical Resistivity Investigations*

Resistivity profiles (9 VES stations) measured with an ABEM Terrameter, SAS 300C, were used for the study. The VES stations were located at least 20 m intervals from one another, except where the landscape was reserved (Figure 3). This interval was applied to attain a high-quality spatial distribution. The Schlumberger array was gradually expanded about a fixed centre and electrode spacing (AB/2) varied from 1 to 80 m and 100 m as the maximum spread length. The VES data were presented as curves of apparent resistivity against AB/2. The observed apparent resistivity data were inverted to a true physical replica of the subsurface using WinRES software (Version 3.0). This technique locates a resistivity image which approximates measured data within the limit of data errors and is in conformity with an area's known geology (Matias et al., 1994). The VES results analysis was used to generate the resistivity-depth curves and spatial resistivity distribution maps. The inversion process created subsurface models that both fit the measured data within error margins and aligned with regional geological knowledge (Matias et al., 1994).

#### *3.1.2 Aeromagnetic Data Processing*

Similarly, four (4) map sheets (Sheet 243-Ilesa, Sheet 244-Ado-Ekiti, Sheet 263-Ondo, and Sheet 264-Akure) of Aeromagnetic survey data were used on a map scale of 1:100,000 series. The data sheets were obtained from the Nigerian Geological Survey Agency. The purposes of using this method are to locate potential geothermal resources, assess subsurface temperature, and also track changes in groundwater flow and understand the faulting processes and distribution of magnetic rocks within the location. The maps were merged and processed into a single dataset and gridded at 0.5 km, and the Spectral Analysis Techniques (SAT) were applied to evaluate the Curie point depth (CPD) around the Ikogosi area and environs. The SAT techniques converted the spatial data into the frequency data domain. Later, a relationship between the average power spectrum of the magnetic anomalies and depths to the corresponding sources is established. The CPD obtained was used to calculate temperature gradients for each profile (block) by the supposition that rocks are dominated by magnetite and using the average thermal conductivity (TC) of 2.5 $mWK^{-1}$ for igneous rock and a Curie

temperature value of 580°C (Tanaka et al. 1999). Consequently, by dividing the temperature by depths, the estimated vertical temperature gradients along each block (profiles) with the average vertical temperature gradient for the whole area is 37.69 ˚C/km. The values of heat flow were determined using the TC of rocks relating to the lithology by using Fourier's equation given in Eq. 4:

$$q = k\frac{dT}{dz} \quad (4)$$

where: $q$ is the heat flow and $k$ is the thermal conductivity coefficient.

There are some indirect methods by which heat flow can be determined when no borehole is available, such as from aeromagnetic data, which has been done in this work. A direct method is from the Bottom hole temperature (BHT) data. Potential targets were identified based on the current understanding of the subsurface imaging and characteristics of the field.

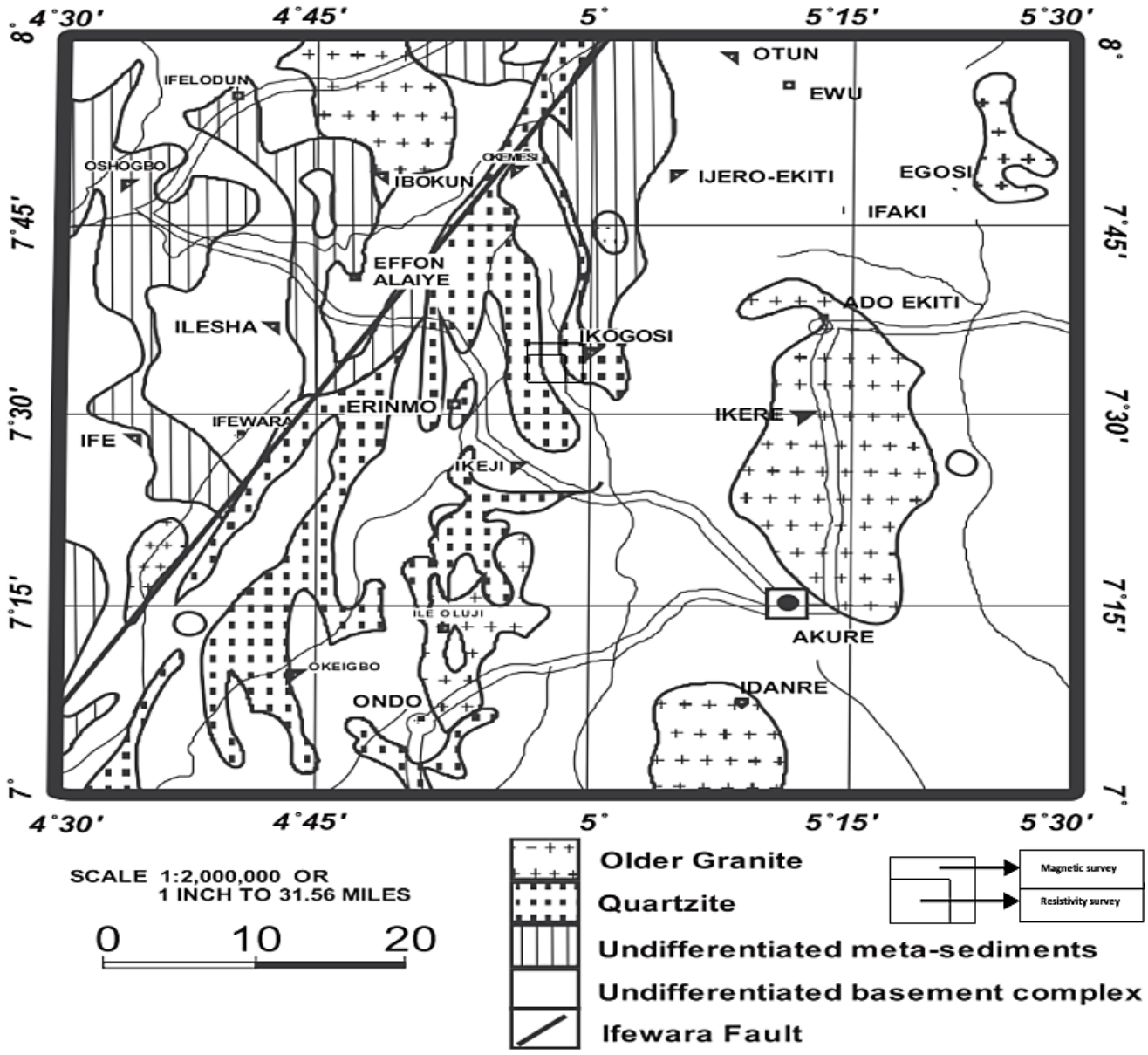


**Figure 2:** Geological map of the Ikogosi Warm Spring and environs (after Abraham et al., 2014).

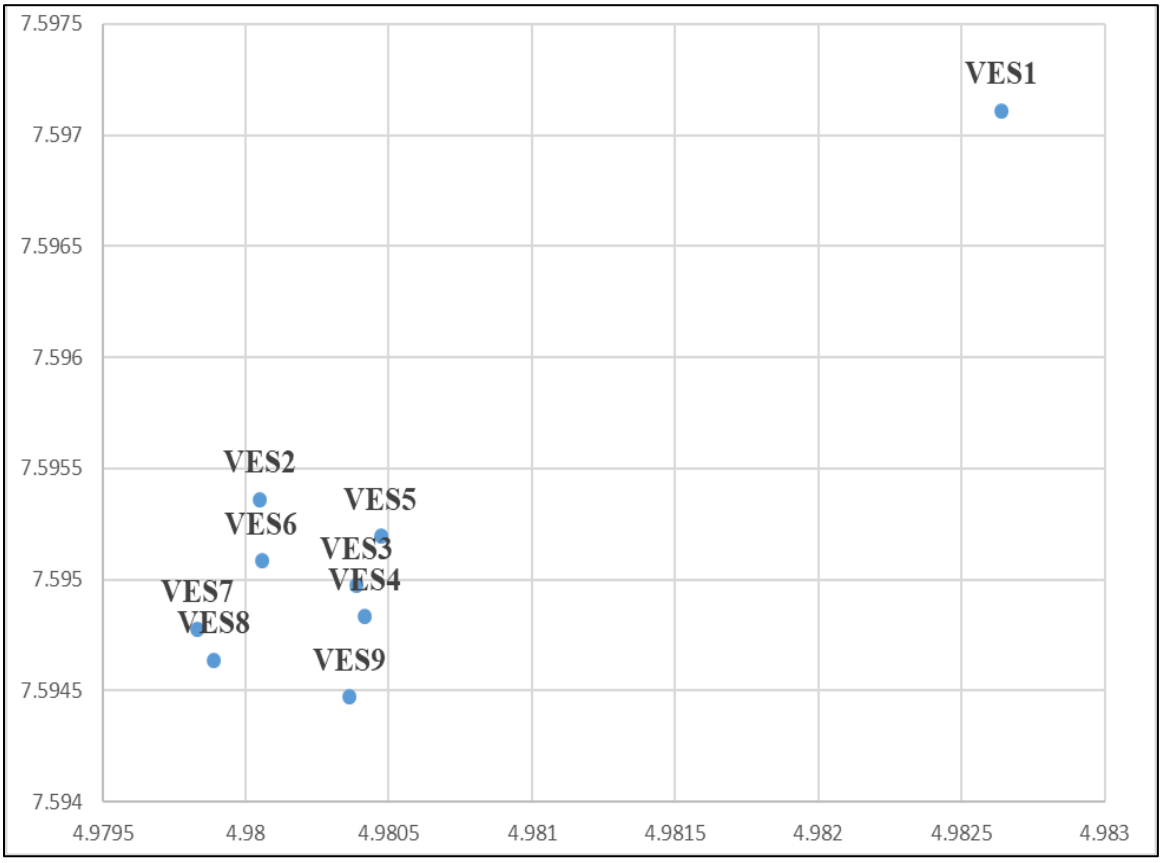


**Figure 3:** Location and position of VES stations of the study area.

## 4. Results and Analysis

The inverted resistivity profiles in the study area have revealed fluid distribution and migration path within the active faults and fractures. The description of the respective resistivity transverses, distributions, and implications is discussed below. The VES curves and maps are displayed in Figures 4 and 5. The electrical fragment outlined four to six subsurface layers composed of topsoil, weathered layers, fresh quartzite, partially fractured quartzite, fractured/faulted quartzite, and fresh quartzite bedrock. The small resistivity zones begin at VES 7-9 (N-S). The first layer was composed of silt, clayey sand, and sand; its thickness ranged between 0.6 and 2.9 m, while resistivity ranged from 34 to 852.9 Ωm. The second layer (fresh quartzitic basement) has a variable thickness (1.5-42.7 m), resistivity ranging from 1.0-1035.2 Ωm. This layer acted as a compacted layer above the first layer in most points. The third layer (fractured quartzite) forms the main aquifer unit because of its thickness, which varied from 2.8 to 66.8 m. The fourth layer (fresh quartzite) had 1.7–2540.3 Ωm resistivity (Table 1). The depth to the top of the fresh quartzite ranged from 7.7 to 75.9 m. The fifth layer (Fresh quartzite) has a resistivity ranging from 1.7-1109.9 Ωm with a depth of 24.6 m and a thickness of 15.8 m. The fresh quartzite bedrock constituted the major bedrock, being the sixth layer, and had 448.6 Ωm resistivity. Figures 12 and 13 represent apparent resistivity maps produced from the VES data for 100 m half current-electrode separation (AB/2). The map reveals high resistivity value (62.5-1082.8 Ωm, i.e., VES 1-3, which is typical of fresh massive quartzite) on the western flank and a higher resistivity (83.7-2540.3 Ωm, i.e., VES 4-6, also typical of fresh quartzite) on the eastern flank and a moderately low resistivity value (1.0-658.3 Ωm i.e VES 7-9 which is characteristic of fractured quartzite) on the southern flank.

Generally, a low resistivity value is a feature of usual geothermal surroundings where hot fluid circulates within the reservoir and finds its way to the surface through a connecting path. Also, the low resistivity observed in VES 1 and 2 may perhaps be due to the occurrence of the hot springs, which, in theory, increases their conductivity. The hot fluid (86.5 - 840.7 Ωm) follows a path between the fault zones. However, the high resistivity in the near surface (VES 4, 5, and 6) can be ascribed to the rock extension and outcropping within the hot springs from field observations. It is assumed that the fault region exists between high-resistivity rock bodies.

The water from the spring is distinctive among known springs occurring in the crystalline hydrogeological zone of Nigeria and even outside Nigeria because of the presence of two major chemical elements of sodium and bicarbonate. The sodium is released by weathering from the host rocks, since it is not present in the atmosphere except as particulate matter, having a concentration range of 0.8 to 20.0 mg/l and 5.0 mg/l as the average concentrations (Sedara and Alabi, 2021; 2022; Talabi, 2013; Talabi et al., 2014). The water from the spring has 5.33 mg/l of sodium, which is a little higher than the average concentrations in meteoric water. This Sodium may perhaps not have been leached from within the thin weathered mantle on the site of the spring, which then implies that it can only come from the earth's interior through fractures in the fresh crystalline rocks. The other element making the spring so unique is its high content of Bicarbonates ($HCO_3$) with a concentration value of 160.8 mg/l, which is approximately five times higher than the

regular concentration in meteoric water. This Bicarbonate has two likely sources, which are atmospheric carbon dioxide dissolved by rainfall water, and the second is carbon dioxide present in the humus soil, which is absorbed by water during permeation (Schoeneich, 2001). This hypothesis is not enough to validate the high content of Bicarbonates in Ikogosi warm spring. Therefore, it means that the warm water from the spring is not just meteoric water; it must have another origin or source, which might likely be volcanoes that are located within the Younger Granite region. Taking into consideration the average geothermal gradient in crystalline hydrogeological zones of Nigeria at only 1.8ºC/100m (Schoeneich and Askira, 1990) and with allowance for cooling on its course upwards, the depth from which the water is coming from must be greater than 1 km since the temperature of the spring water is around 39.8ºC which suggests that the water originates from a great depth.

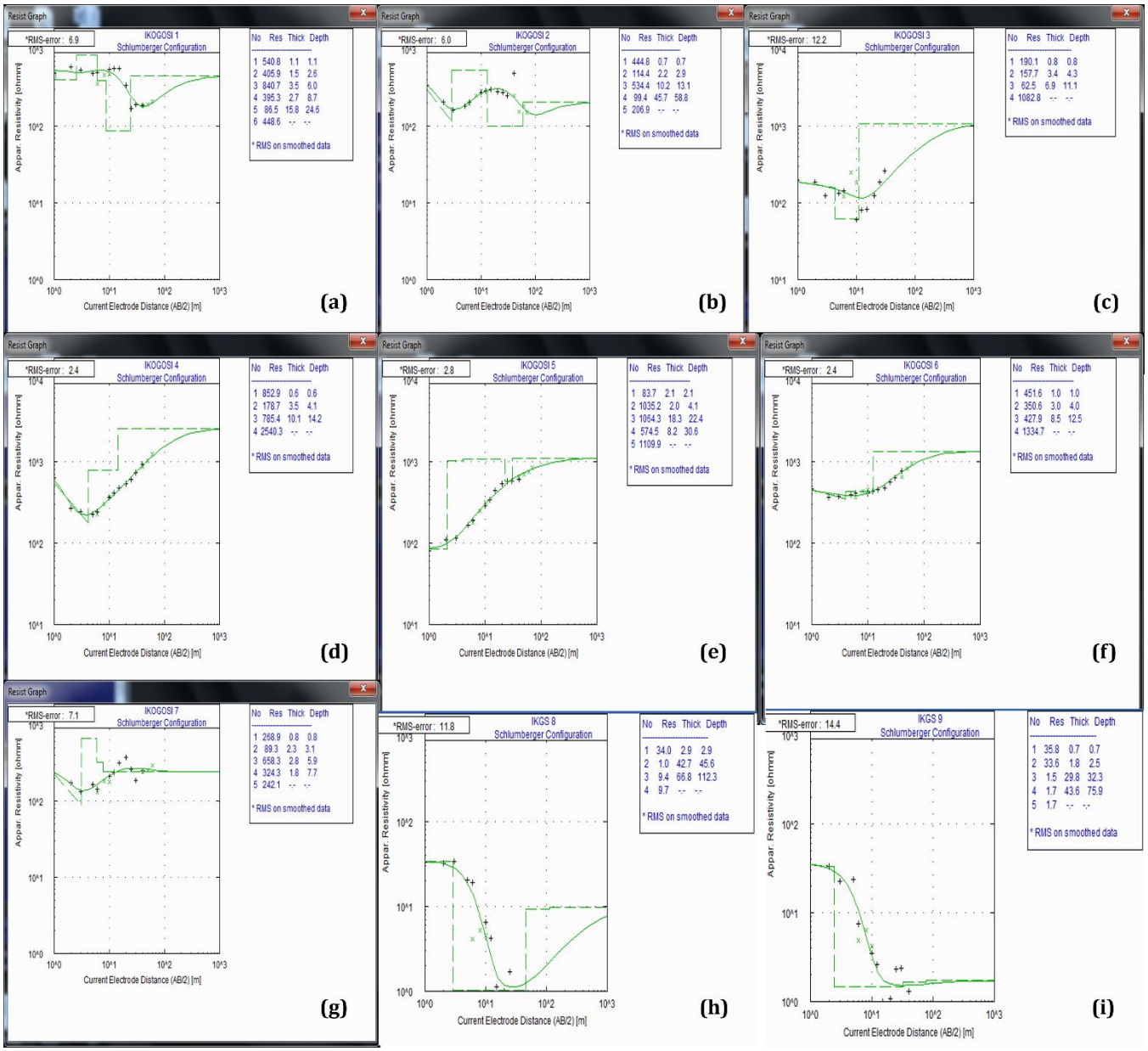


**Figure 4:** (a) Layer model interpretation of VES1 (warm section), (b) VES2 (warm section), (c) VES3 (warm section), (d) VES 4 (cold section), (e) VES 5 (cold section), (f) VES 6 (cold section), (g) VES 7 (mixed section), (h) VES 8 (mixed section), and (i) VES 9 (mixed section).

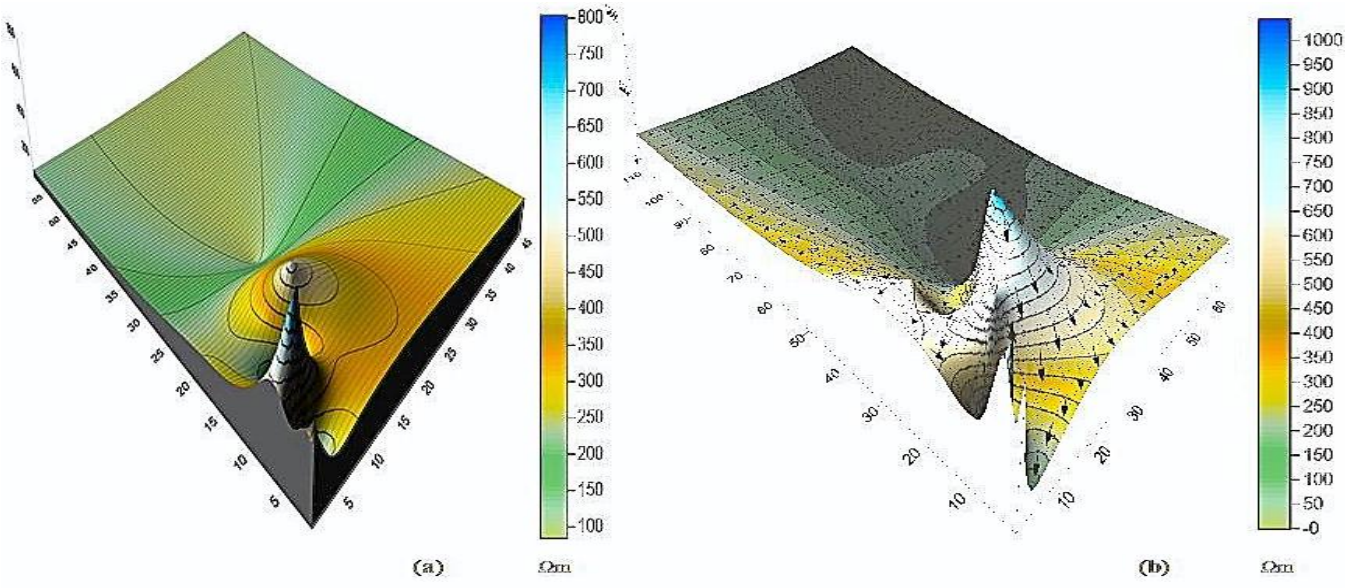


**Figure 5:** 3D contour map of resistivity variations with depth and thickness for (a) VES 1-3, and (b) whole study area.

**Table 1:** Average resistivity and depth value of all profiles.

| VES | Latitude | Longitude | Average resistivity (Ωm) | Average depth (m) |
|---|---|---|---|---|
| 1 | 7.597111 | 4.982639 | 453.0 | 8.6 |
| 2 | 7.595361 | 4.98005 | 279.98 | 18.9 |
| 3 | 7.594972 | 4.980389 | 373.3 | 5.4 |
| 4 | 7.594833 | 4.980417 | 1089.3 | 6.3 |
| 5 | 7.595194 | 4.980472 | 773.5 | 14.8 |
| 6 | 7.595083 | 4.980056 | 641.2 | 5.83 |
| 7 | 7.594778 | 4.979833 | 316.6 | 4.4 |
| 8 | 7.594639 | 4.979889 | 13.5 | 56.9 |
| 9 | 7.594472 | 4.980361 | 14.9 | 27.9 |

### *4.1 Heat flow and Temperature Estimation to Depth from Aeromagnetic data*

Estimation of the temperature profile to 5 km is a very important factor in the geothermal energy assessment of an area. This 5km depth option is considered a cut-off for commercialization and exploitation of geothermal energy (Chopra and Holgate 2005). In lieu of drilling and direct measurements in wells at depth, heat flow modeling provides a basis for reasonably accurate estimation of temperatures to depth. In a purely conductive heat regime, the descending approximation and assessment of steady-state temperature to a depth $z$ can be performed by:

$$T_z = T_o + q_o \int_o^z \frac{d_z}{k_z} \quad (5)$$

where: $k_z$ is thermal conductivity of the interval, $d_z$ = interval thickness, $q_o$= heat flow at the top of the interval $T_o$ and $T_z$ = temperature at the top and bottom of the interval, respectively.

Equation 5 is a first-order calculation when there are no in-situ measurements at depth, which is an overview of a multifarious dynamic system. These established thermal conductivity profiles and conductive modeled heat flow values were then used to estimate temperatures to 5 km using equation (5). The temperatures estimated at 5 km depth ranged between 110 and 250°C. Based on the temperature estimations, the Ikogosi, Effon Alaye, Ikere, Ijero, and Erinmo units were identified as high prospective units for geothermal energy (Table 2).

Conventional heat flow data in Nigeria is very scarce, most especially for the southwestern region of Nigeria. This data is available in the works of Brigaud and Lucazeau (1985) from the West Africa Shield (Nigeria, Ghana, and Liberia) with values ranging between 30-40 $mWm^{-2}$ and the works of Verheijen and Ajakaiye (1979) with an average value of 38.5 $mWm^{-2}$. The heat flow estimation in Southwest Nigeria has been through CPD estimation and assuming a constant Curie temperature and rock Thermal conductivity value. Hence, most of the heat flow data available around Nigeria was either acquired through aeromagnetic data or well logging. In the absence of conventional heat flow and thermal conductivity characteristics and description of the rocks in the above area, it is very difficult to arrive at the variations of reported heat flow from the actual heat flow of the regions.

The CPD estimated for the IKGWS area varied between 12 and 21 km and mean value of 16 km. Similarly, the heat flow values for the area varied between 75 and 127 $mW/m^2$, and the mean value of 100 $mW/m^2$, while the temperature gradient varied between 28 and 48 °C/Km and the mean value of 38 °C/Km. Figure 3 shows the heat flow map of the entire area, and the IKGWS area is located at the bottom right corner. There can

be no in-depth deductions from limited measurement. Therefore, it is necessary to have direct measurements from Bottom hole temperatures (BHT) from boreholes (temperature-depth data) in the IKGWS area, which will be reliable than the computational approach done in this work for the CPD (Figure 6).

### *4.2 Typical model for the Ikogosi geothermal system*

The reservoir consists of different perpendicular sets of highly permeable fractures that cross-cut the low-permeable formations. These fractures are completely clogged near the surface. The mostly conductive heat exchanges of the reservoir with the surface are thus reduced by thermal blanketing, the total leakage of the geothermal fluid at the surface (both terrestrial and rainwater) being estimated to be only between 25–30 °C (Figure 7). Convection cells are active within the aquifer, ensuring its thermal and geochemical homogeneity. Thus, three major and essential factors explain the existence and location of the IKGWS field: a heat source (magmatic source), a network of permeable fractures at the origin of the geothermal aquifer, and an impermeable surface cover, limiting energy loss and ensuring the durability of the fluid.

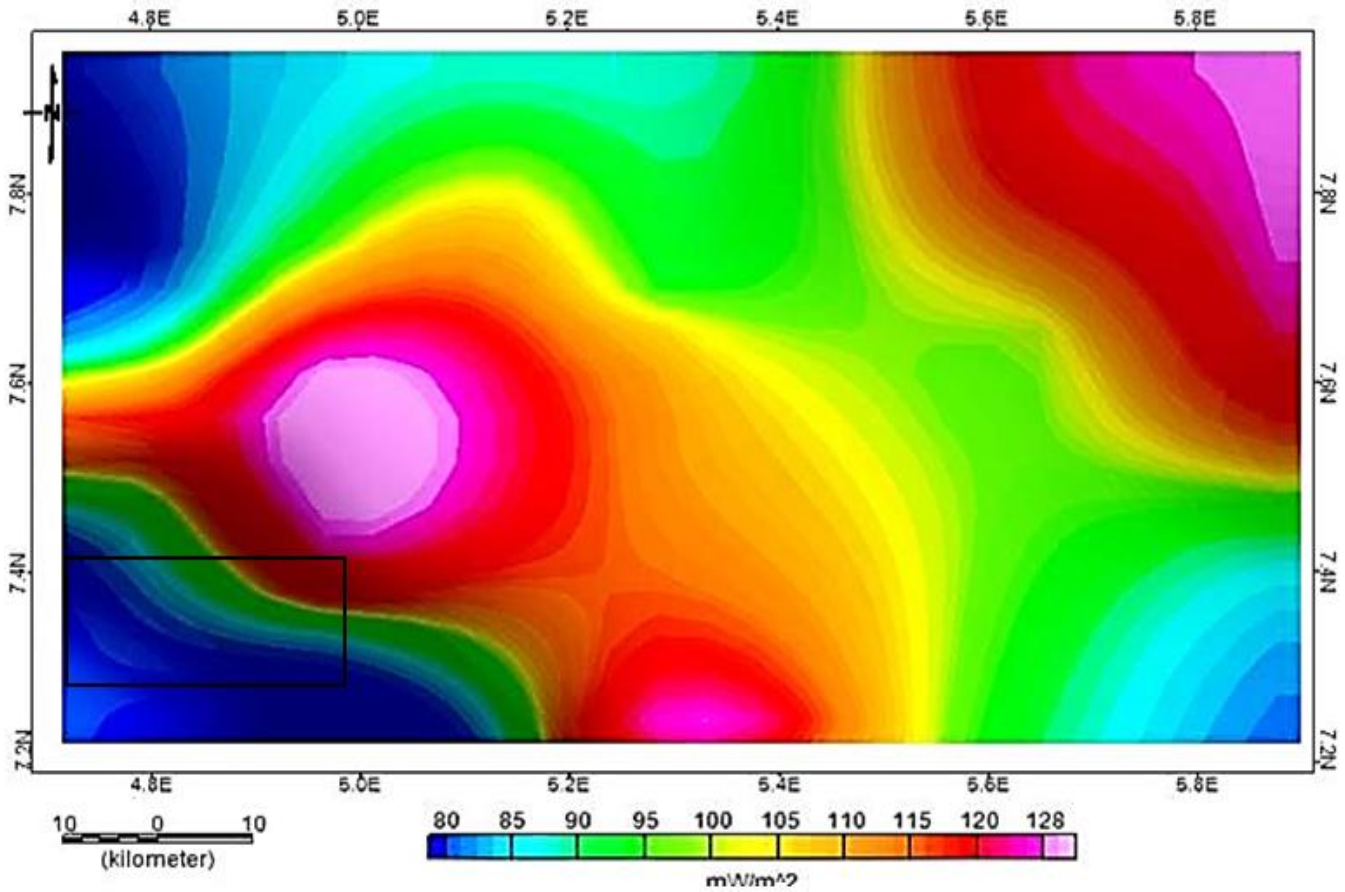


Figure 6: Heat flow map of the study area. The study area is indicated in a black rectangular polygon.

## 5. Conclusion

This study underscores the efficacy of combining resistivity and aeromagnetic methods to investigate geothermal systems. Applied to the Ikogosi Warm Spring in Ekiti State, southwestern Nigeria, these techniques revealed subsurface geothermal structures and fluid dynamics. Low-resistivity zones identified through resistivity analysis correlate with fractured/faulted quartzite regions, interpreted as conduits for deep-seated geothermal groundwater migration to the surface. Persistently low resistivity values within the geo-electric sections confirm upward fluid migration along fault systems. The integrated surveys contributed critically by mapping geothermal anomalies with identification of low-resistivity zones (e.g., VES 7–9) as conduits within Pliocene sediments, marking target areas for potential steam exploitation. Also, by characterizing the subsurface architecture by defining basement depth, thickness, and hydraulic properties governing surface water discharge. These findings highlight fractured quartzite/faulted zones (notably VES 7–9) as prime targets for geothermal energy exploration, where enhanced permeability facilitates fluid ascent from deep reservoirs.

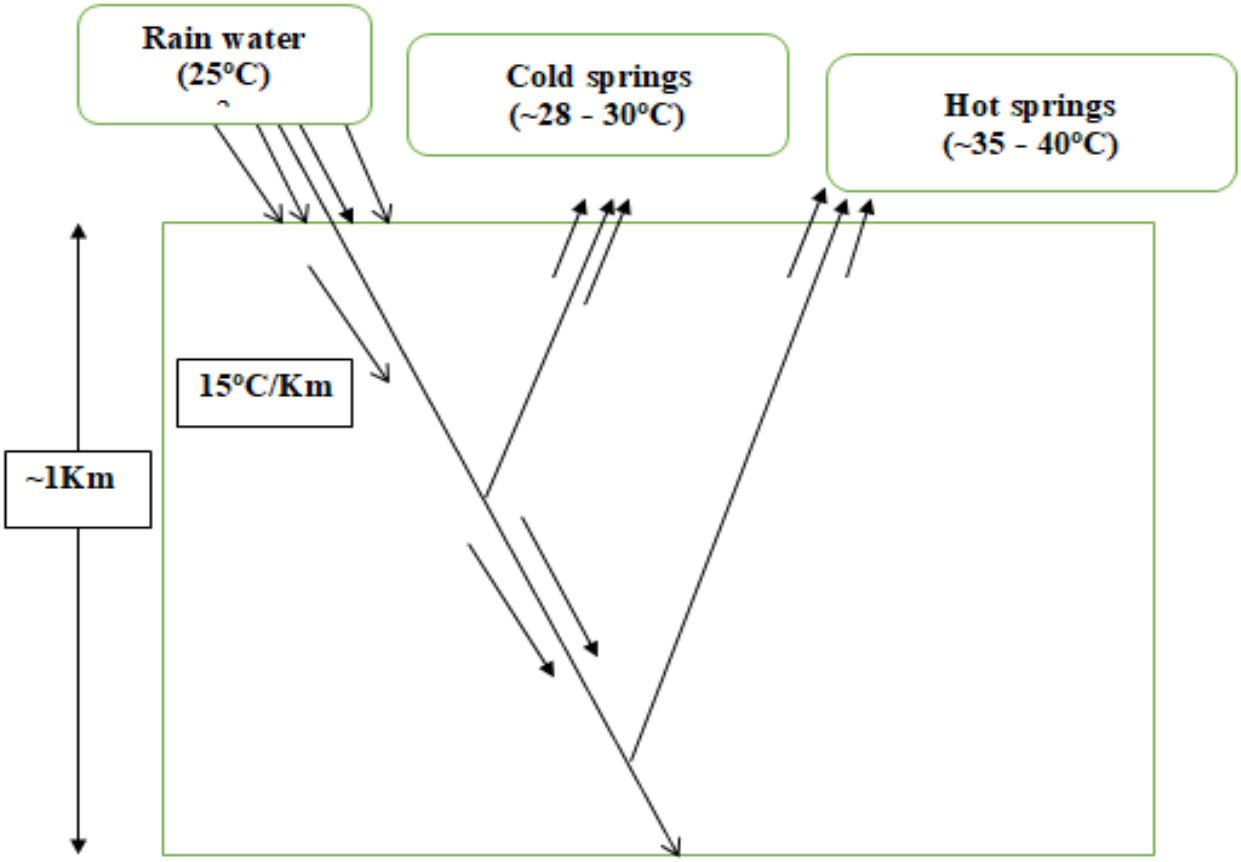


**Figure 7:** Typical model of the Ikogosi geothermal system.

**Table 2:** CPD and Heat flow computation for the Ikogosi spring and surrounding area.

| Tectonic Unit | Locality | Zb (km) | TG (°C/km) | HF ($mW/m^2$) | RSA ($k/m^2$) | RD (kg/m3) | RSHC (J/kg°C) |
|---|---|---|---|---|---|---|---|
| UBC | Ilesa | 20.59 | 28.17 | 74.64 | 10 | 2800 | 1000 |
| UBC | Ilesa | 15.48 | 37.46 | 99.27 | 15 | 2600 | 1000 |
| QUARTZITE | Erinmo | 13.5 | 42.98 | 113.89 | 10 | 2800 | 1000 |
| UBC/QUARTZITE/UBC | Effon Alaye | 14.36 | 40.4 | 107.06 | 10 | 2800 | 1000 |
| UBC/QUARTZITE/UBC | Effon Alaye | 16.44 | 35.29 | 93.52 | 15 | 2600 | 1000 |
| QUARTZITE | Ado-Ekiti | 14.58 | 39.77 | 105.39 | 10 | 2800 | 1000 |
| QUARTZITE | Ado-Ekiti | 16.42 | 35.32 | 93.59 | 10 | 2600 | 1000 |
| UBC | Ijero | 13.48 | 43.02 | 114.01 | 10 | 2800 | 1000 |
| UBC | Ijero | 15.16 | 38.26 | 101.38 | 10 | 2600 | 1000 |
| UBC | Akure | 16.33 | 35.51 | 94.1 | 10 | 2800 | 1000 |
| UBC | Akure | 20.36 | 28.49 | 75.49 | 10 | 2800 | 1000 |
| UMC | Ondo | 16.17 | 35.88 | 95.08 | 10 | 2600 | 1000 |
| UMC | Ondo | 15.41 | 37.63 | 99.73 | 5 | 2800 | 1000 |
| UBC/OLDER GRANITE | Ikere | 17.5 | 33.14 | 87.82 | 5 | 2600 | 1000 |
| UBC/OLDER GRANITE | Ikere | 13.81 | 41.99 | 111.27 | 5 | 2800 | 1000 |
| UMS/QUARTZITE | Ikogosi | 12.13 | 47.82 | 126.71 | 6 | 2800 | 1000 |
| UMS/QUARTZITE | Ikogosi | 16.78 | 34.56 | 91.58 | 10 | 2600 | 1000 |
| UBC | Ilesa | 16.36 | 35.46 | 93.97 | 10 | 2800 | 1000 |
| UMS | Osogbo | 14.24 | 40.72 | 107.92 | 5 | 2800 | 1000 |
| UMS | Osogbo | 13.81 | 42 | 111.3 | 5 | 2600 | 1000 |

*TG=Temp. Grad.; HF= Heat flow; RSA= surface area of Resource; RD=density of rock; RSHC= specific heat capacity of rock, UMS=Undifferentiated meta-sediments; UBC=Undifferentiated basement complex*

## Acknowledgments

The author is grateful to all the anonymous reviewers whose contributions and comments have greatly improved this manuscript.

## Funding

This research received no specific grant from any funding agency in the public, commercial, or not-for-profit sectors.

## Competing Interest

The author affirms that there are no identifiable conflicts of interest, either financial or personal, that could be perceived as influencing the work presented in this paper.

## Data Availability Statement

All data generated or analyzed during this study are included in this published article.

## Ethics Approval

No human or animal specimens were used in this research.

## References

Abdullahi, M., Adagunodo, T. A., and Ehinola, O. A. (2023). Magnetotelluric evidence for deep heat source beneath Ikogosi geothermal system, Nigeria. *Journal of African Earth Sciences,* 198, 104812.

Adagunodo, T. A., Sunmonu, L. A., and Ehinola, O. A. (2022). Hydrogeophysical assessment of Ikogosi spring discharge dynamics. *Environmental Earth Sciences*, 81(4), 112.

Adegbuyi, O., and Abimbola, A. F. (1997). Energy resource potential of Ikogosi Warm Spring Area, Ekiti State, Southwestern Nigeria. *African J Sc* 1(2):111–117.

Adegbuyi, O., Ajayi, O.S. and Odeyemi, I.B. (1996). Prospects of Hot-Dry-Rock (HDR) geothermal energy resource around the Ikogosi warm spring in Ekiti state, Nigeria. *J. Renew. Energy*, 4:58-64.

Allis, R. G. (1990). Geophysical anomalies over geothermal fields. *Geothermics,* 19(3), 211-239. https://doi.org/10.1016/0375-6505(90)90002-3

Anderson, E., Crosby, D., Ussher, G. (2000). Bulls-eye- Simple resistivity imaging to reliably locate the geothermal reservoir. Proc. World Geothermal Congress 2000, Kyushu-Tohoku, Japan, May 28- June 10, 2000, 909-914.

Andrés, J., Eggenkamp, H. G. M., and García-López, S. (2020). $\delta^{18}O$ and $\delta^{2}H$ constraints on the origin of geothermal fluids in continental collision zones. *Geothermics,* 88, 101891.

Aneke, M., Agbajor, F. D., and Ogunribido, T. H. (2022). Caprock integrity in West African geothermal systems: A comparative review. *Renewable Energy,* 195, 1352–1365.

Archie, G. E. (1942). The electrical resistivity log as an aid in determining some reservoir characteristics. *Transactions of the AIME*, 146(1), 54-62. https://doi.org/10.2118/942054-G

Arnason, K., Krlsdottir, R., Eysteinsson, H., and Flovenz, O.G. (2000). The resistivity structure of high temperature geothermal systems in Iceland. Proc. World Geothermal Congress, 2000. Kyushu-Tohoku, Japan, p. 923-928.

Battistel, M., Hurwitz, S., Evans, W. C., and Barbieri, M. (2021). Meteoric water recharge in geothermal systems: Global isotopic evidence. *Applied Geochemistry,* 134, 105073.

Brigaud, F., and Lucazeau, F. (1985). Heat Flow from the West African Shield. *Geophysical Research Letters*, 12(9):549-552, September 1985.

Caby, R., and Boesse, J.M. (2001). Pan-African Nappe system in south west Nigeria; the Ife-Ilesha schist belt. *Journal of African Earth Sciences* 33 (2), 211-225.

Chopra, P., and Holgate, F. (2005). A GIS analysis of temperature in the Australian crust, *Proceedings,* World Geothermal Congress 2005, Antalya, Turkey.

Cumming, W., Mackie, R., and Tullar, J. (2020). Resistivity/MT for geothermal exploration: Best practices and case studies. *GRC Transactions,* 44, 1-15.

Ehinola, O. A., Adagunodo, T. A., and Olabode, O. P. (2021). Lithium-silica geothermometry of Ikogosi springs: Implications for hybrid fluid sources. *Journal of Geochemical Exploration*, 231, 106864.

Flovenz, O. G., Spangenberg, E., Kumlenkampf, J., Arnasson, K., Karlsdottir, R., Huengens, E. (2005). The role of electrical interface conduction in geothermal exploration. World Geothermal Congress 2005, Antalya, Turkey. April 24-29.

Fridleifsson, G. O., Elders, W. A., and Albertsson, A. (2021). The Iceland Deep Drilling Project: Radiogenic vs. magmatic heat sources in continental rifts. *Geothermics,* 96, 102221.

Garba, M.L., Kurowaska, E., Schoeneich, K. and Abdullahi, I. (2012). Rafin Rewa Warm Spring: A new geothermal discovery. *American International Journal of Contemporary Research*, 2(9).

Grant, M. A., and Bixley, P. F. (2023). Fractured geothermal reservoirs*:* Porosity-permeability relationships (2nd ed.). Elsevier.

Hairul, A. H., Ismail, B., and Abidin, M. H. Z. (2013). Rainwater percolation vs. magmatic fluids in geothermal systems: Isotopic case studies. *Geothermal Energy,* 1(1), 1–15.

Samrock, F., Kuvshinov, A., Bakker, J., Jackson, A., and Fisseha, S. (2015). 3-D analysis and interpretation of magnetotelluric data from the Aluto-Langano geothermal field, Ethiopia. *Geophysical Journal International*, 202(3) 1923–1948, https://doi.org/10.1093/gji/ggv270

Matias, M. S., Macques da Silva, M., Ferreira, P., and Ramallio, E. (1994). A geophysical and hydrogeological study of aquifers contamination by a landfill. *J. Applied Geophysics* 32: 155-162.

Mielke, P., Bär, K., and Sass, I. (2022). Precambrian-hosted geothermal systems: A global review. *Earth-Science Reviews*, 234, 104234.

Olabode, O. P. (2023). Thermal anomalies in Nigerian springs: New temperature datasets from 2018–2022. *Data in Brief,* 48, 109204.

Schoeneich, K. (2001). Water Resources Management. Unpublished Lecture Notes, Ahmadu Bello University, Zaria.

Schoeneich, K., and Askira, M.T. (1990). Water resources of the Lake Chad Basin, Nigeria. Water Resources. *J Nigerian Assoc Hydrogeol* 2(1).

Sedara, S.O., and Alabi, O.O. 2022. Heat flow Estimation and Quantification of Geothermal Reservoir of a Basement Terrain using Geophysical and Numerical Techniques. *Environ Earth Sci* ***81****,70* (Springer) *https://doi.org/10.1007/s12665-022-10201-6*

Sedara, S.O., and Alabi, O.O. (2021). Geothermal prospect scaling of Ikogosi warm spring using combined geophysical methods. *J. Indian. Geophys. Union, 25(5):55-70.*

Talabi, A. O. (2013). Hydrogeochemistry and Stable Isotopes (δ18O and δ2H) Assessment of Ikogosi Spring Waters. *American Journal of Water Resources* 1, no. 3 (2013): 25-33. doi: 10.12691/ajwr-1-3-2.

Talabi, A. O., Afolagboye, O. L., Tijani, M. N., Aladejana, J. A. and Ogundana, A. K. (2014). Hydrogeochemistry of Some Selected Springs' Waters in Ekiti Basement Complex Area, Southwestern Nigeria. *International Journal of Engineering and Science,* 3(2):19-30.

Tanaka, A., Okubo, Y., and Matsubayashi, O. (1999). Curie point depth based on spectrum analysis of the magnetic anomaly data in East and Southeast Asia. *Tectonophysics* 306, 461–470.

Ussher, G., Harvey, C., Johnstone, R., and Anderson, E. (2000). Understanding the resistivities observed in geothermal systems. *Transactions-Geothermal Resources Council*, 24, 585-590.

Verheijen, P.T., and Ajakaiye, D.E. (1979). Heat-flow measurements in the Ririwai ring complex, Nigeria. *Tectonophysics* 54:T27–T32.

Zonge, K. L., Hughes, L. J., and Carlson, N. R. (2005). Resistivity techniques in geothermal exploration. In M. H. Powers (Ed.), *Geothermal exploration techniques* (pp. 145-182). Society of Exploration Geophysicists.

**How to Cite:** Sedara, S.O. (2025). A combined interpretation of electrical resistivity and airborne magnetic datasets for assessment and evaluation of a geothermal reservoir in South West Nigeria. *Science Research Annals–Physical Sciences,* 1(1), 24–33. https://doi.org/10.63112/e79ke582